



SOLPS-ITER simulations of an X-point radiator in the single-null and snowflake divertor configurations in ASDEX Upgrade and EU-DEMO



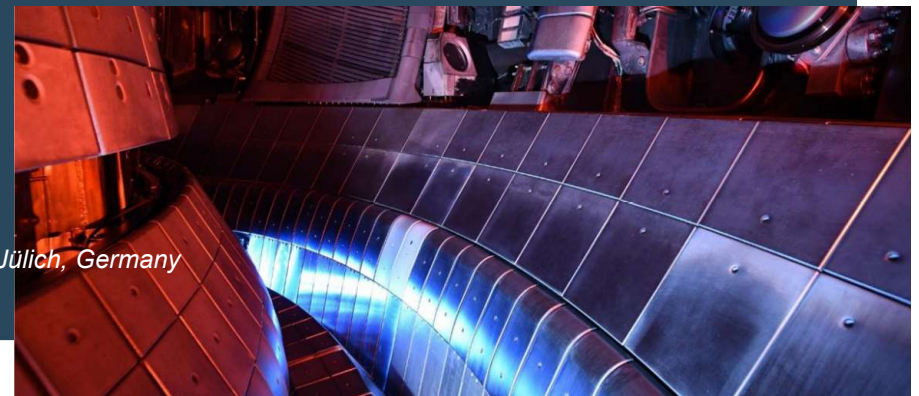
O. Pan¹, M. Bernert¹, T. Lunt¹, M. Cavedon², S. Wiesen³,
M. Wischmeier¹, U. Stroth^{1,4} and the ASDEX Upgrade team

¹Max-Planck-Institut für Plasmaphysik, 85748 Garching, Germany

²Dipartimento di Fisica "G. Occhialini", Università di Milano-Bicocca, Milan, Italy

³Forschungszentrum Jülich GmbH, Institut für Energie- und Klimaforschung-Plasmaphysik, Jülich, Germany

⁴Physik-Department E28, Technische Universität München, Garching, Germany



Outline



Motivation & Introduction

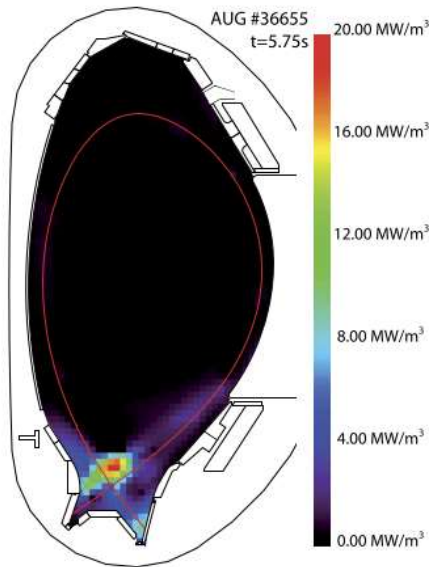
SOLPS-ITER modeling for an X-point radiator

The access condition of an XPR – comparison with the reduced model [Stroth, NF, 22]

Preliminary study on machine-size dependence

Summary

X-point radiator

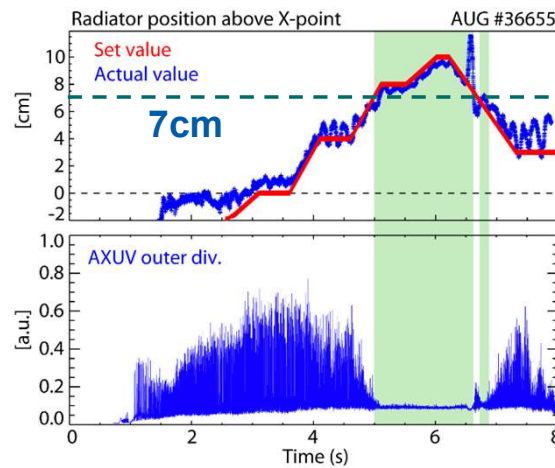


[Bernert, NF, 2021]
[Bernert, PSI, 2022]



X-point radiator: a stable, localized and highly radiative region near the X-point inside the confined plasma in metallic machines AUG and JET.

ELM suppression with moderate confinement degradation when the XPR is deep enough inside the confined region.



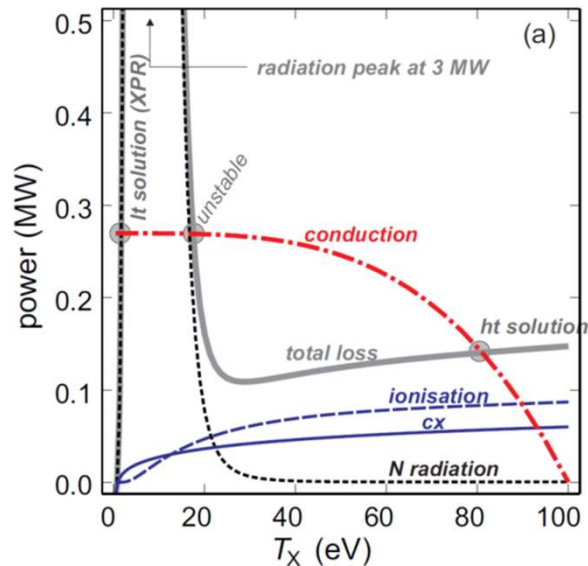
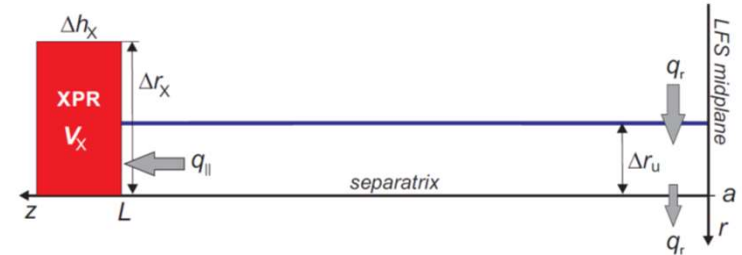
- Viable reactor scenario**
- Full detachment
 - $\geq 90\%$ radiation
 - ELM suppression
 - Acceptable confinement
 - Easy control
 - Compatible with power changes

A reduced model for the initiation of an XPR

An XPR occurs when

$$X_A = \frac{P_I + P_{CX}}{P_{cond}} \approx \frac{(2\langle\sigma v\rangle_I + \langle\sigma v\rangle_{CX})}{(2/7)\hat{\kappa}_e} \cdot \frac{L_c f_{exp} \Delta h_X B_{t,u}}{B_{\theta,u}} \cdot \frac{n_{e,u}}{T_{e,u}^{2.5}} \cdot n_{0,X} > 1$$

[Stroth, NF, 2022]



Highlight the role of

- Neutrals
- Magnetic connection length & flux expansion

Neutral density at the X-point → hard to measure in experiments

Spatial distribution of particle and energy sources

Cross-field transport, drifts, HFS/LFS asymmetry



2D numerical simulations

Outline



Motivation & Introduction

SOLPS-ITER modeling for an X-point radiator

The access condition of an XPR – comparison with the reduced model [Stroth, NF, 22]

Preliminary study on machine-size dependence

Summary

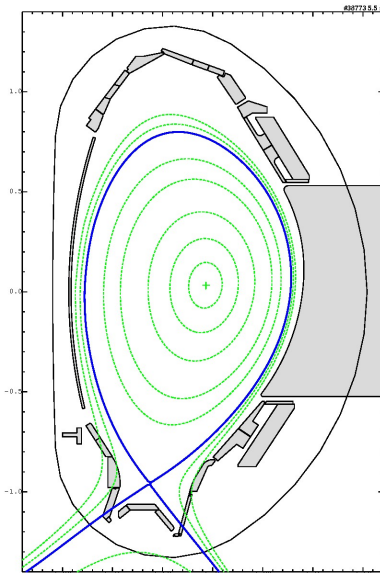
SOLPS-ITER simulation for an XPR



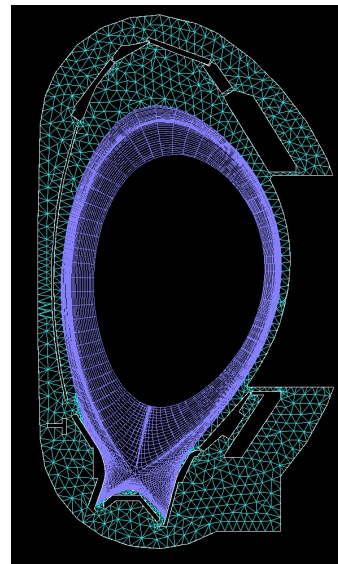
SOLPS-ITER code package:

- B2.5 (2D multi-fluid plasma transport code)
- EIRENE (kinetic Monte Carlo neutral particle transport code)

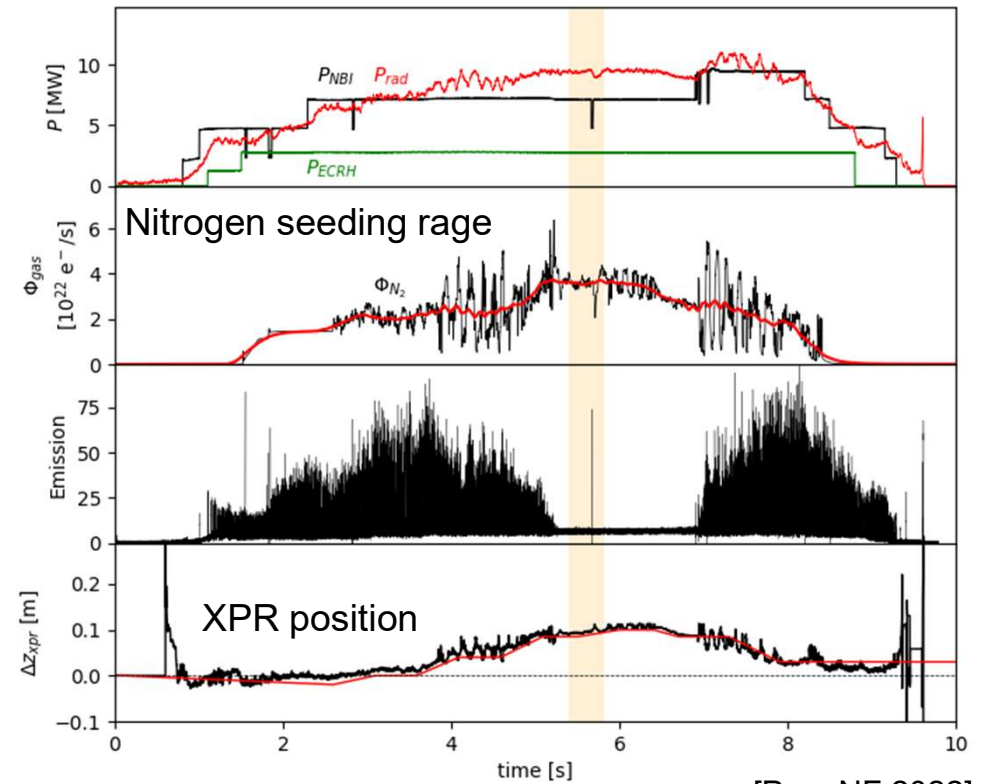
Equilibrium



SOLPS-ITER grids

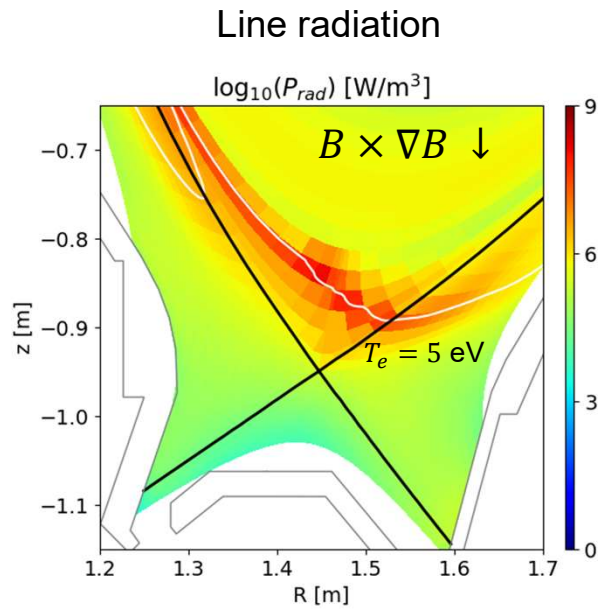


AUG #38773



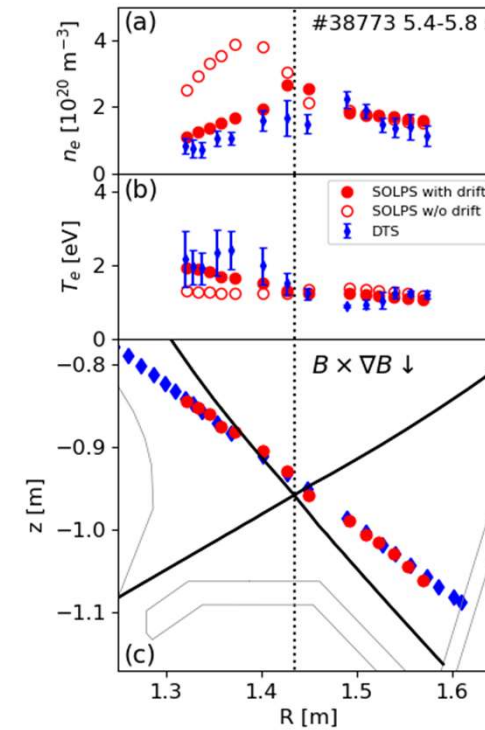
[Pan, NF 2022]

SOLPS-ITER simulation for an XPR



In the confined region near the X-point:

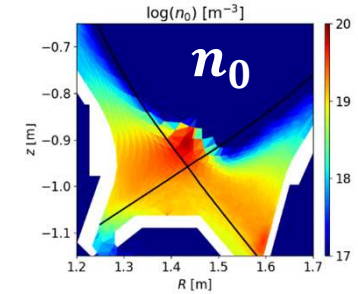
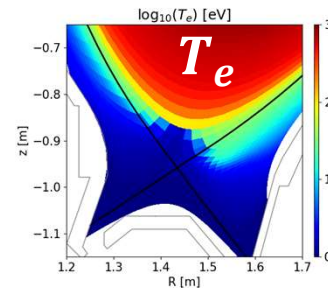
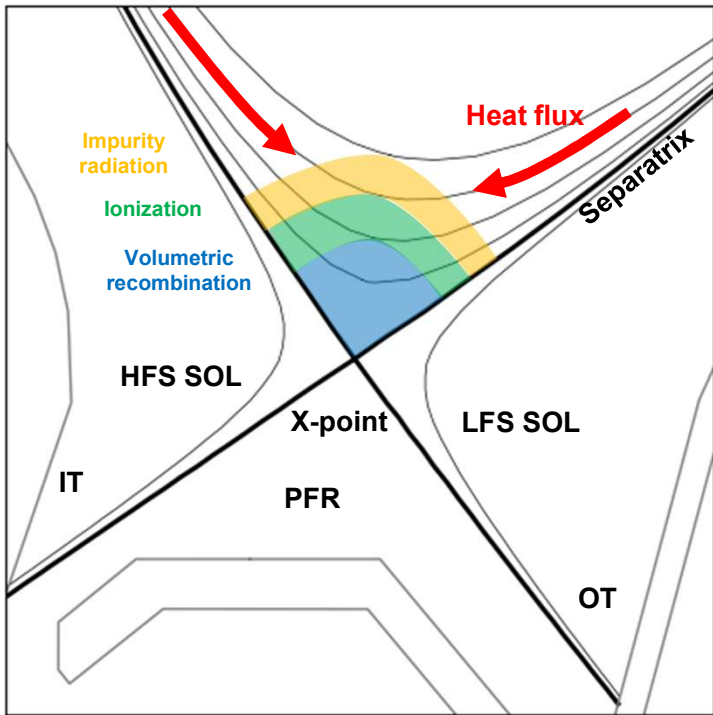
- A highly radiative band
- A cold XPR core ($T_e < 5 \text{ eV}$)



[Pan, NF 2022]

Good agreements with the divertor Thomson scattering measurements

A simple sketch of XPR in SOLPS-ITER simulations

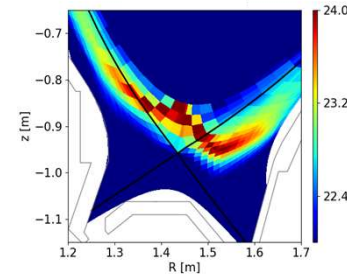


Increased neutral density at the X-point

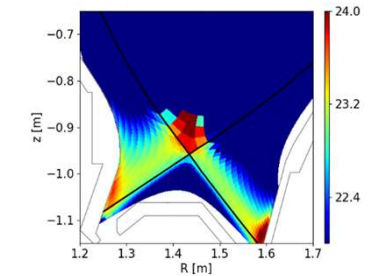
Ionizing region with $T_e \sim 10$ eV

Recombining region with $T_e \sim 1$ eV

Ionization rate



Volumetric recombination rate



Outline



Motivation & Introduction

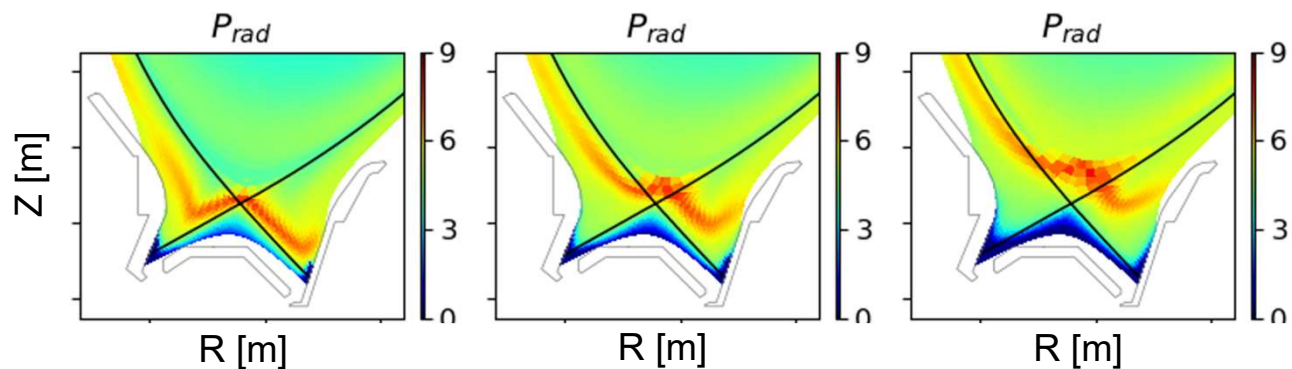
SOLPS-ITER modeling for an X-point radiator

The access condition of an XPR – comparison with the reduced model [Stroth, NF, 22]

Preliminary study on machine-size dependence

Summary

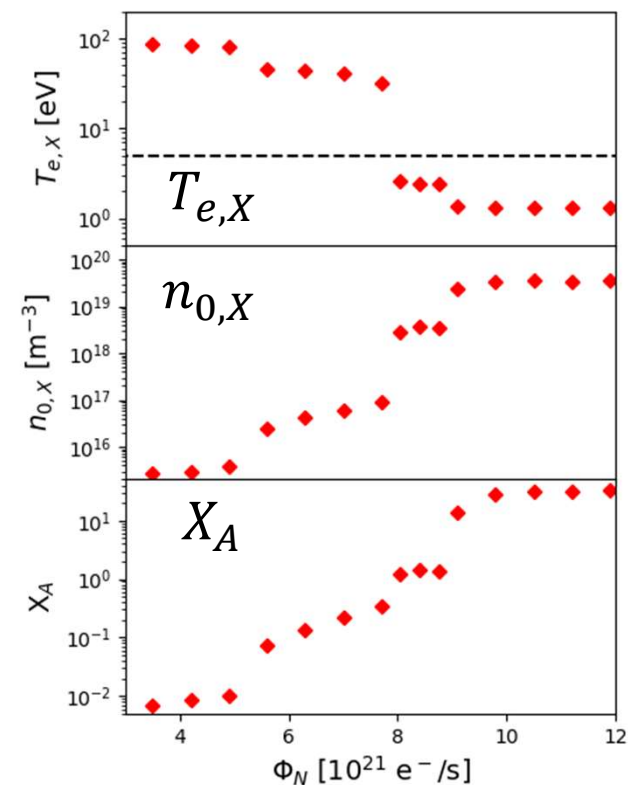
The formation of an XPR in SOLPS-ITER simulations



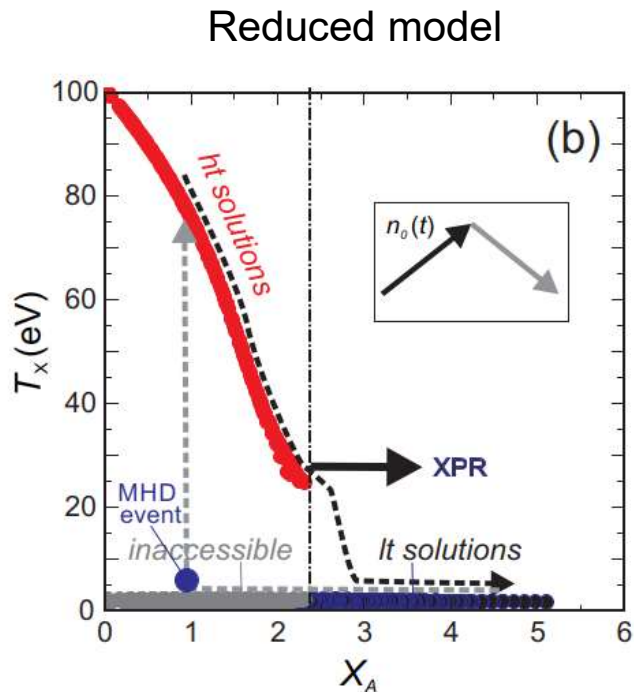
$\Phi_N = 5.6 \times 10^{20} e^-/s$
 $\Phi_N = 8.4 \times 10^{20} e^-/s$
 $\Phi_N = 1.1 \times 10^{21} e^-/s$

With increasing nitrogen impurity seeding rate:

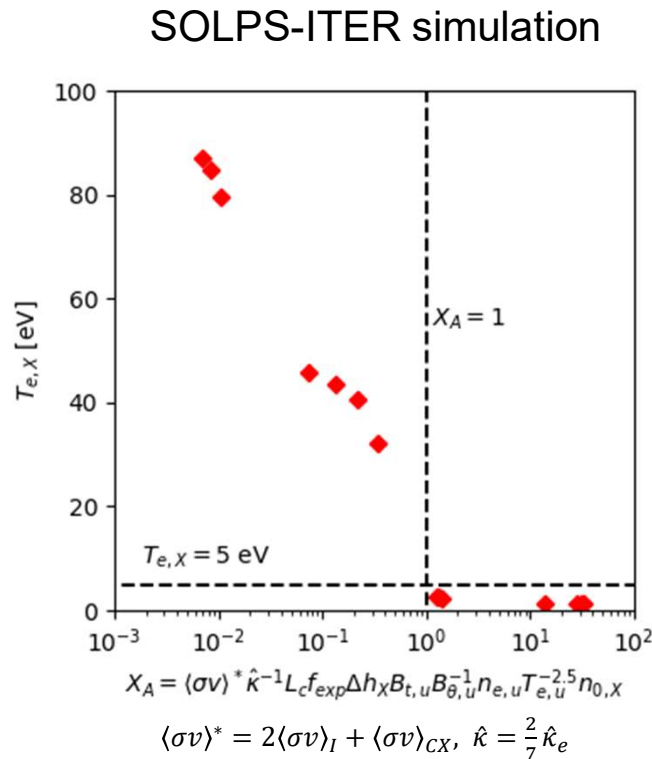
- Electron temperature decreases at the X-point
- Neutral density increases at the X-point
- X_A increases



XPR access condition – comparison with the reduced model



[Stroth, NF, 2022]



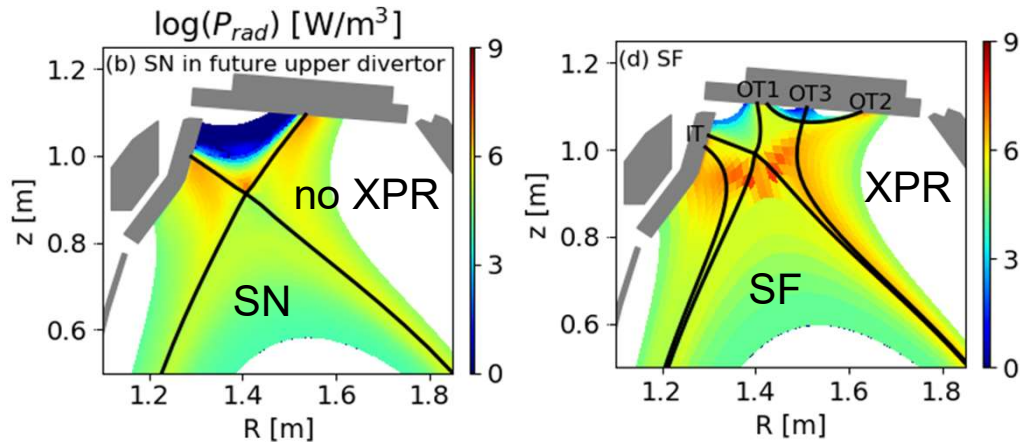
An XPR ($T_{e,x} < 5$ eV) occurs with $X_{A,threshold} \sim 1$

Good agreements with the reduced model

Only a rough estimate, while parameter dependencies are more robust

$$X_A = \frac{P_I + P_{CX}}{P_{cond}} \approx \frac{(2\langle\sigma v\rangle_I + \langle\sigma v\rangle_{CX})}{(2/7)\hat{\kappa}_e} \cdot \frac{L_c f_{exp} \Delta h_X B_{t,u}}{B_{\theta,u}} \cdot \frac{n_{e,u}}{T_{e,u}^{2.5}} \cdot n_{0,X}$$

SOLPS-ITER modeling for the future upper divertor of AUG

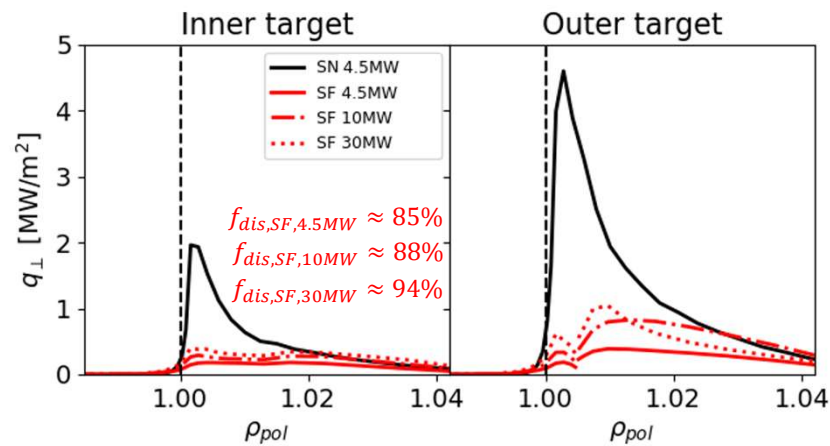


With similar upstream profiles and N seeding rate:

$$\text{SN: } X_A = 0.004, \quad n_{0,X} = 7 \times 10^{15} \text{ m}^{-3}$$

$$\text{SF: } X_A = 1.2, \quad n_{0,X} = 5 \times 10^{17} \text{ m}^{-3}$$

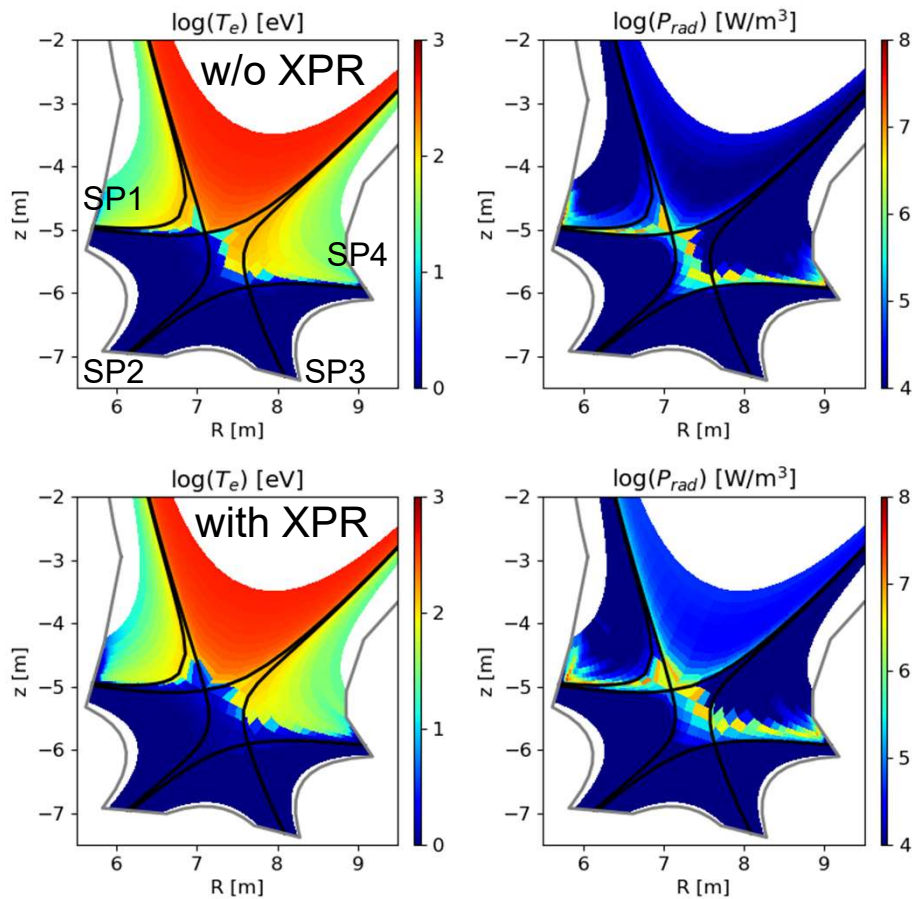
Easier access of an XPR in a snowflake divertor
(larger connection length and larger flux expansion)



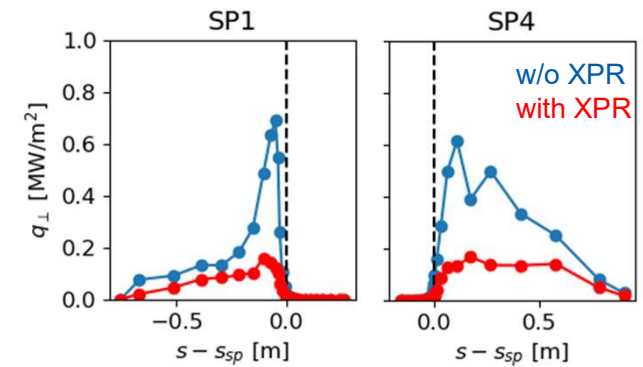
$$X_A \approx \frac{(2\langle\sigma v\rangle_I + \langle\sigma v\rangle_{CX})}{(2/7)\hat{\kappa}_e} \cdot \frac{L_c f_{exp} \Delta h_X B_{t,u}}{B_{\theta,u}} \cdot \frac{n_{e,u}}{T_{e,u}^{2.5}} \cdot n_{0,X}$$

Withstanding a power increase by a factor of 6

SOLPS-ITER modeling for DEMO SFD



Reduced target heat fluxes with an XPR



Without XPR:

$$T_{e,u} = 209 \text{ eV}, n_{e,u} = 3.0 \times 10^{19} \text{ m}^{-3}, Z_{eff,ompsep} = 1.03$$

$$T_{e,X} = 97 \text{ eV}, n_{0,X} = 1.9 \times 10^{15} \text{ m}^{-3}, X_A = 0.37$$

With XPR:

$$T_{e,u} = 183 \text{ eV}, n_{e,u} = 2.5 \times 10^{19} \text{ m}^{-3}, Z_{eff,ompsep} = 1.08$$

$$T_{e,X} = 2.7 \text{ eV}, n_{0,X} = 2.3 \times 10^{17} \text{ m}^{-3}, X_A = 4.7$$

The X_A threshold also roughly works for DEMO SFD

Outline



Motivation & Introduction

SOLPS-ITER modeling for an X-point radiator

The access condition of an XPR – comparison with the reduced model [Stroth, NF, 22]

Preliminary study on machine-size dependence

Summary

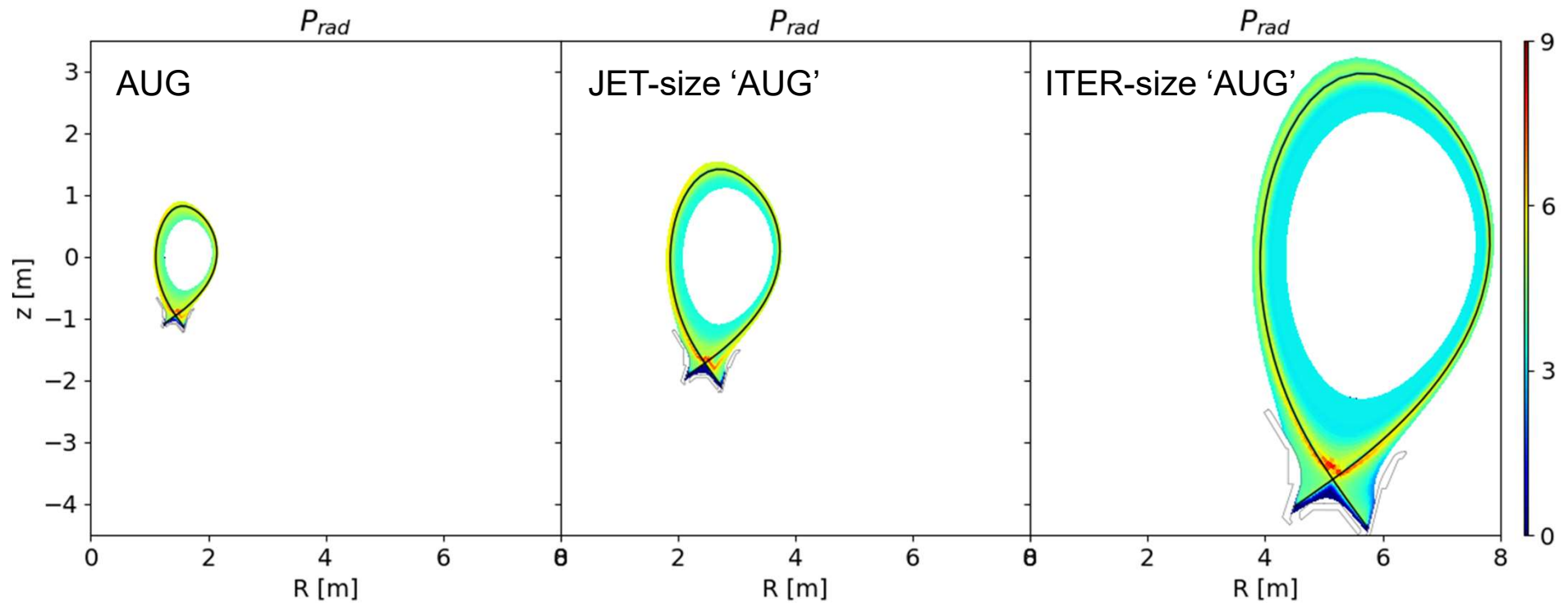
Preliminary study on machine-size dependence

Keeping the same separatrix and divertor shapes

Varying the major radius

Comparing simulations with a similar $T_{e,X}$

	R_0 [m]	P_{in} [MW]	I_p [MA]	B_T
AUG	1.65	5	0.8	2.5
JET-size	2.96	21	2.5	3.0
ITER-size	6.20	105	12	5.3



Preliminary study on machine-size dependence

Simulation results in the flux tube with $T_{e,X} \approx 1.4$ eV

	$B_{t,u}/B_{\theta,u}$	f_{exp}	$n_{e,u}$ [10^{19}m^{-3}]	$T_{e,u}$ [eV]	$n_{0,X}$ [10^{19}m^{-3}]	X_A
AUG	5.3	36	3.1	65	2.5	1.7
JET-size	4.0	36	3.2	106	3.4	1.3
ITER-size	3.1	36	2.4	112	1.8	1.2

Similar X_A value with different machine-size

Good agreement with the reduced model

$$X_A \approx \frac{(2\langle\sigma v\rangle_I + \langle\sigma v\rangle_{CX})}{(2/7)\hat{\kappa}_e} \cdot \frac{L_c f_{exp} \Delta h_X B_{t,u}}{B_{\theta,u}} \cdot \frac{n_{e,u}}{T_{e,u}^{2.5}} \cdot n_{0,X} \sim R_0^2 q_s^2 f_{exp} n_{e,u} T_{e,u}^{-5/2} n_{0,X}$$

Outline



Motivation & Introduction

SOLPS-ITER modeling for an X-point radiator

The access condition of an XPR – comparison with the reduced model [Stroth, NF, 22]

Preliminary study on machine-size dependence

Summary

Summary



SOLPS-ITER modeling is able to reproduce the X-point radiator phenomenon in AUG and showed good agreements with experimental measurements.

The simulations also showed consistency with the reduced model for the initiation of an X-point radiator [Stroth, NF 2022].

The simulations highlight the important role of neutrals, magnetic connection length & flux expansion in the initiation of an XPR.

